

SODIUM DIFFUSION, SELENIZATION, AND MICROSTRUCTURAL EFFECTS ASSOCIATED WITH VARIOUS MOLYBDENUM BACK CONTACT LAYERS FOR CIS-BASED SOLAR CELLS

John H. Scofield

Physics Department, Oberlin College, Oberlin, OH 44074

and

S. Asher, D. Albin, J. Tuttle, M. Contreras, D. Niles, R. Reedy, A. Tennant, and R. Noufi

National Renewable Energy Laboratory, 1617 Cole Blvd., Golden, CO 80401

ABSTRACT

By varying the argon pressure during deposition, we have prepared a set of sputtered molybdenum films on soda-lime glass substrates with a range of mechanical and electrical properties. These films were subsequently exposed to several of the processing steps used in the fabrication of copper-indium-diselenide (CIS) solar cells. Processing steps of interest include heating in a vacuum, exposure to selenium vapor at elevated temperatures, and deposition of CIS and CIGS layers over the Mo. Resulting Mo films and structures were subsequently characterized using XPS, SEM, Auger, and SIMS. Here we describe the results of these experiments and their implications for CIS cell fabrication.

INTRODUCTION

Over the last several years the conversion efficiency achieved by the "best" polycrystalline thin film copper indium diselenide (CIGS) based small-area solar cells has risen to above 16% [1, 2, 3]. While the efficiencies of the "best" small-area cells have steadily improved, uncontrolled factors continue to thwart the reproducibility of these cells, and to a greater extent, degrade the quality and through-put of large-area CIS and CIGS module fabrication efforts. In connection with these problems, a variety of suspect areas have been suggested; these include 1) the nature and importance of surface defects on the glass substrates, 2) substrate cleaning processes, 3) the possible formation of MoSe₂ near the Mo/CIS interface, 4) the possible importance of sodium diffusion into the CIS, 5) the softening of the glass substrate at the high processing temperatures, and 6) adhesion failures at the Mo/glass and/or Mo/CIS interfaces [4].

A number of these issues appear to be related to the properties of the Mo back contact layer universally employed for CIS and CIGS devices. At most institutions, and particularly at NREL, considerable fabrication efforts have been devoted to improving the properties of the absorber layer. In contrast, significantly less effort has been devoted to understanding and shaping the properties of the Mo layer. In many cases, the Mo layer has been deposited by whatever means were available, with the only property of concern being the Mo sheet resistance. Only recently have we recognized importance of the Mo layer as the substrate

upon which the CIS absorber layer is grown and that it may have significant impact on the absorber layer nucleation, growth, and morphology.

The electrical and mechanical properties of sputtered refractory metal films are known to vary with sputter pressure [5]. We have used this fact to fabricate a set of Mo films on soda-lime glass substrates with widely varying properties. The resulting films have been characterized using several analytical techniques including XPS, SEM, SIMS, XRD, and GIXRD (glancing-incidence XRD). We have also measured film resistivity and adhesion to the glass substrate. In order to shed light on some of the questions raised above we have subjected these Mo films to our usual solar cell processing stages, including the high-temperature deposition of CIS and CIGS and the completion of solar cells.

In this paper we describe the results of these experiments and discuss their implications for CIS and CIGS solar cell fabrication.

AS-DEPOSITED FILMS

Sample Fabrication

Films were sputter-deposited onto 2 in. x 2 in. x 0.095 in. soda-lime glass substrates held approximately 8 cm from a 12 cm x 20 cm, planar, dc magnetron, Mo target. Substrates were cleaned using our standard soap/DI water scrub and rinse process. After cleaning, substrates were blown dry with N₂ gas and immediately loaded into the vacuum chamber that was subsequently evacuated to a base pressure near 1×10^{-6} Torr. Two substrates were coated during one pump-down. The details of the deposition process may be found elsewhere [6]. For our first set of experiments a set of seven, roughly 500-nm-thick Mo films were sputtered at Ar pressures (P) of 0.2, 0.5, 1.0, 2.0, 5.0, 10, and 20 mTorr respectively. Deposition rates were approximately 1 nm/s.

Stress and Resistivity

Film resistivity (ρ) and in-plane stress (σ) are shown in Figs. 1 and 2, the latter determined from GIXRD measurements [6]. The figures show that films deposited at low Ar pressure have low resistivity and compressive stress. As the pressure is increased, the resistivity

increases and stress becomes tensile. At the highest pressures, the resistivity continues to increase while the magnitude of the stress falls back towards zero, again becoming compressive at the highest pressure. The

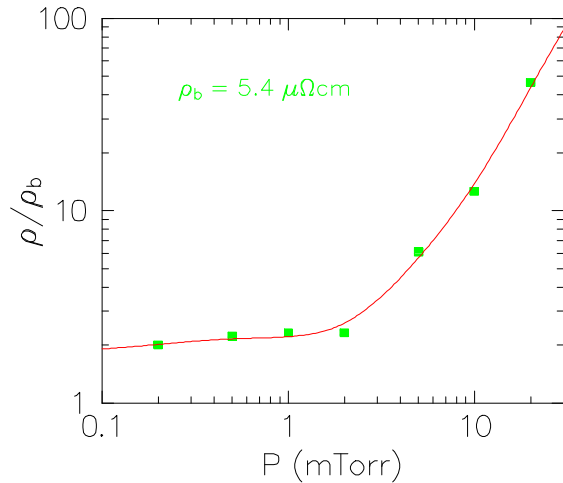


FIG. 1 Graph of the normalized, room-temperature film resistivity, ρ/ρ_b , versus Ar pressure during sputtering. The curve is a guide to the eye.

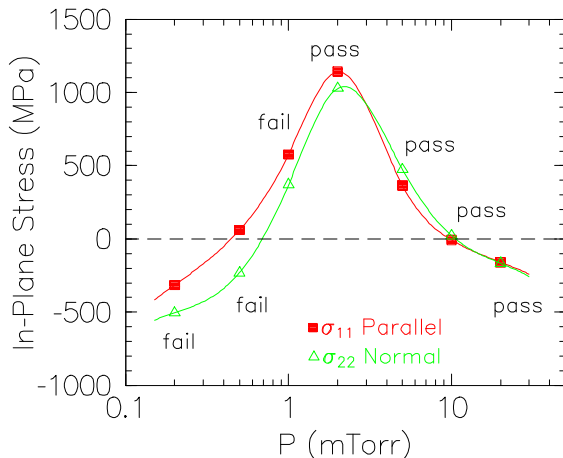


FIG. 2 In-plane stresses plotted against Ar pressure; negative values indicate compression while positive values indicate tension. Tape test results for adhesion are also indicated.

results are consistent with those reported for other sputtered refractory metal films [5]. It is also important to note that films sputtered at the three lowest pressures exhibited poor adhesion, failing the tape test (see Fig. 2).

As Figs. 1 and 2 show, films sputtered at low Ar pressure have the lowest resistivity while those sputtered at high pressures exhibit the best adhesion. We have developed a bilayer process that captures the best of both worlds. This process involves the deposition of a thin (~100 nm) layer at high Ar pressure immediately followed by a thicker (~900 nm) layer deposited at low Ar pressure. Such films achieve low resistivity and good adhesion and have been incorporated into NREL's high-efficiency cells [6].

SUBSEQUENT PROCESSING

Experimental Method

Since films sputtered at lower pressures did not adhere well to the glass, we decided not to submit the above films to subsequent processing steps, which would place even higher demands on film adhesion. To minimize variations associated with adhesion, we fabricated a second set of Mo films, each of these films having a bilayer structure, with the properties of the 900-nm-layer being varied. Also, so that differences in subsequent properties could be directly related to the original Mo films, we decided to restrict our attention to only four Mo films, and to process these four samples simultaneously in future experiments, thereby eliminating the effects of possible hidden, uncontrolled variables. This second set of samples consisted of 1- μ m-thick Mo bilayers with the first, 100-nm-thick layer deposited at 10 mTorr and the second, 900-nm-thick layer sputtered at $P = 0.5, 2, 5,$ and 10 mT respectively. Samples were subdivided into smaller pieces, and sets of four (one for each P) were processed together for subsequent experiments. Table I lists the various experimental conditions.

Results

SEM characterization of the as-deposited Mo films show that they all have columnar grain structure. Films deposited at low pressure are more dense with "closed" grain boundaries while those deposited at higher pressures are less dense with more "open" grain boundaries. These features qualitatively explain the variation of resistivity and stress with sputter gas pressure [5].

SIMS depth profiles were used to characterize the concentrations of Na, O, Se, and C or K impurities. Se levels in as-deposited films were negligible.

| Expt. | Description | Subsequent Analysis |
|-------|---|--------------------------------|
| A1 | as deposited | 4-probe, SIMS, SEM, GIXRD, XRD |
| A2 | vacuum anneal for 30 min. @ 450°C | 4-probe, XPS, SIMS |
| B1 | expose to 2 nm/s dep. rate of Se for 15 min @ 450°C | 4-probe, XPS, SIMS |
| D1 | deposit CIS using selenization | XPS, SIMS, SEM |
| E1 | deposit CIGS using 3-stage process | XPS, SIMS, SEM |

TABLE I List of processing steps to which the four Mo bilayer films were submitted along with the characterization methods to which they were subsequently submitted for analysis.

Depth profiles for Na and O impurities for as-deposited films are shown in Figure 3. (For comparison purposes, the depth scales for Figures 3 and 4 have been adjusted to account for variations in film thicknesses.) The O impurity level increases with

sputtering pressure, being approximately 30 times higher in the 10 mT film than in the 0.5 mT film. Sodium levels varied with deposition pressure and depth, being lowest in the interior and highest towards the surfaces of the Mo films.

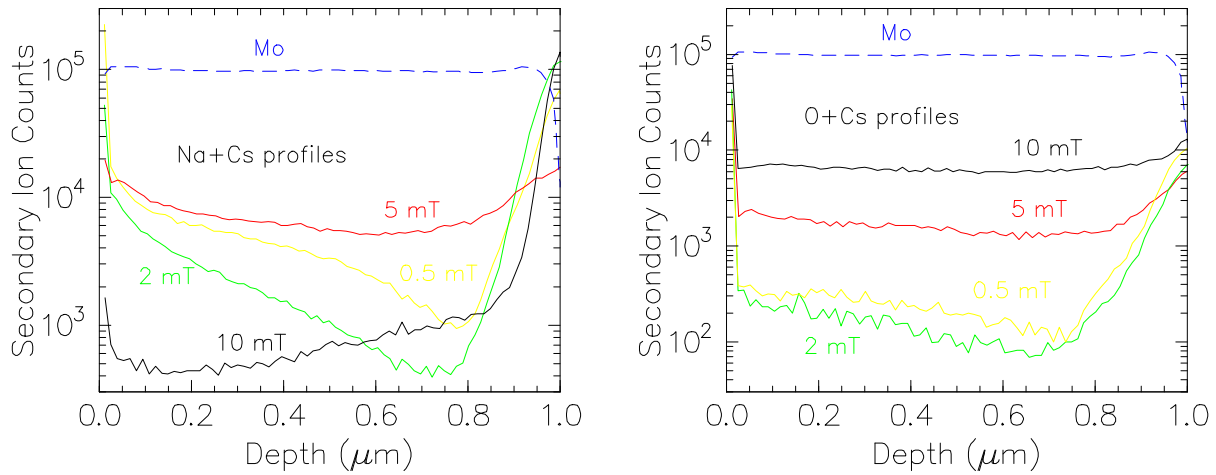


FIG. 3 SIMS data for as-deposited films showing depth profile for a) Na and b) O for the four bilayer Mo films. Also shown for reference is the SIMS signal for Mo.

With subsequent processing at elevated temperatures the Na and Se impurity concentrations changed significantly. Figure 4 shows (a) the Na- and (b) the Se-distributions for films exposed to Se flux at 450 °C. Na profiles changed significantly from those in the as-deposited films indicating significant diffusion,

especially in the higher-pressure Mo films. For all films data show a significant build-up of Na within about 100 nm of the air/Mo interface. Figure 4(b) indicates substantially more selenization for the 10 mT than for the other Mo films.

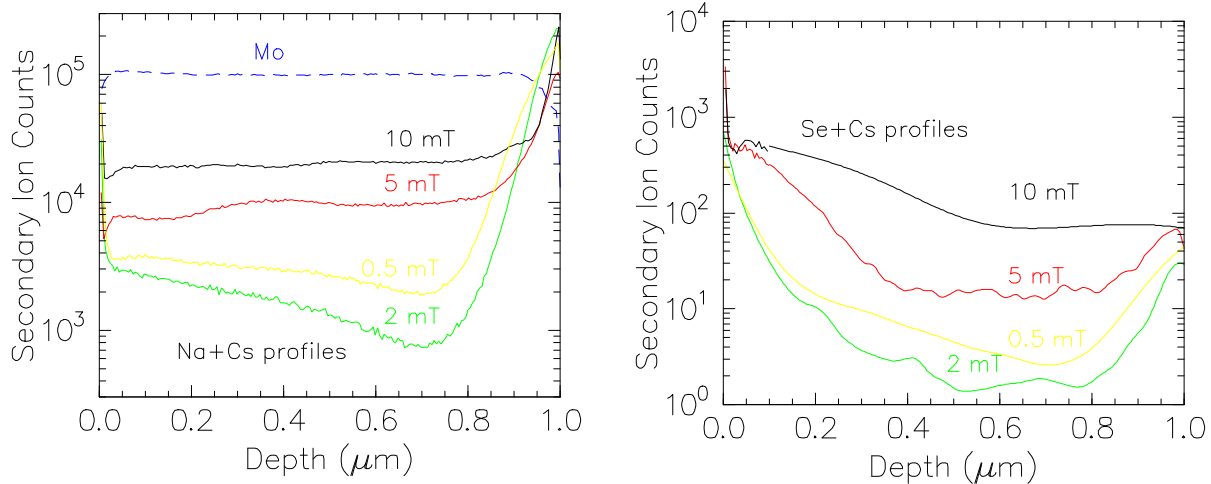


FIG. 4 SIMS data for films exposed to Se flux at 450°C showing depth profiles for a) Na and b) Se. Also shown, for reference, is the SIMS signal for Mo. 2 mTorr and 0.5 mTorr curves have been "smoothed" so that they are distinguishable.

Figure 5 shows the SIMS depth profiles for films following deposition of a CIGS absorber layer using NREL's 3-stage process (experiment E1). Similar data (not shown) have been obtained for films following deposition of a CIS absorber layer via selenization (experiment D1). Note that the depth scale has not been corrected for differences in sputter rates leading to

distortion in the apparent absorber and Mo layer thicknesses.

Of particular interest is the Na depth profile. In the Mo back contact, Na impurity levels and distributions are similar to those of Figure 4, again showing that the low-pressure Mo contains significantly less Na than the high-pressure Mo. Despite these differences, the Na levels in

the four absorber layers appear to be the same, independent of the underlying Mo layers. For all four samples there is significant build-up of Na at both CIGS surfaces. XPS analysis (not shown) indicates that CIS thin films grown with the selenization process have < 1%

Na in the 20 nm region near the air/CIS surface while CIGS films grown using NREL's 3-stage process have more than 10% Na there. Both absorber layers show the build-up of Na at the absorber/Mo interface.

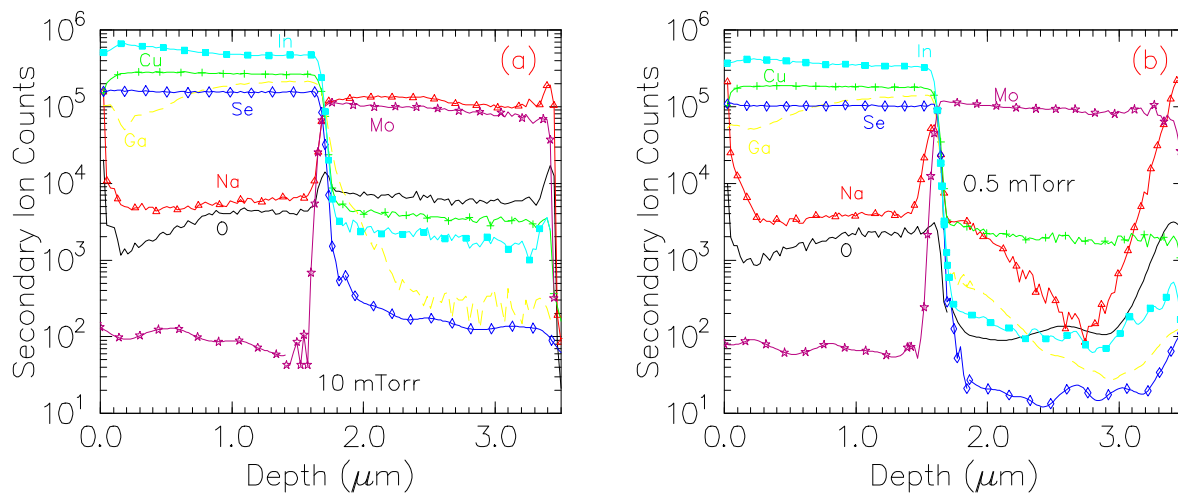


FIG. 5 SIMS data following CIGS deposition using NREL's 3-stage process on Mo sputtered at a) 10mTorr, and b) 0.5 mTorr Ar pressure.

In addition to the data shown, SEM photos suggest that absorber grain size tends to increase with lower Mo deposition pressure, the effect being more pronounced for CIS deposition using selenization than for CIGS deposition using the NREL 3-stage process. In addition, selenized CIS layers appear to adhere better to the high-pressure Mo than to the low-pressure Mo.

DISCUSSION AND CONCLUSIONS

The O, Na, and Se depth profiles, electron micrographs, and Mo resistivity and strain data all suggest that the high-pressure Mo films have smaller grains, a more open grain structure (i.e., larger gaps between grains), and are more porous than the low-pressure Mo films. For the high-pressure Mo this leads to greater inclusion of oxygen (probably in the grain boundaries), higher resistivity, higher Na levels, and more rapid impurity diffusion. The morphology of the high-pressure Mo provides a greater number of nucleation sites for the absorber layer, leading to better absorber adhesion and smaller, less faceted absorber grains. These differences lead to greater selenization of the high pressure Mo during absorber formation (see Figs. 4 and 5).

The Na impurity levels in the absorber, however, appear to be independent of the underlying Mo properties, suggesting that they are determined by thermodynamic rather than kinetic factors. The relatively high Na concentrations at the two CIGS surfaces (air and Mo) are particularly interesting. There is some evidence that Na may play an important role in cell performance [7].

ACKNOWLEDGMENTS

The authors would like to thank J. Dolan for assistance configuring the Mo deposition system, P. Perdicki and B. Ballard for GIXRD measurements, A. Duda for bulk XRD measurements, and R. Matson for SEM characterization. One of the authors (JHS) was supported, in part, by an Associated Western Universities - Department of Energy Faculty Sabbatical Fellowship. This work was performed at NREL under contract No. DE-AC36-83CH10093 to the U. S. Department of Energy.

REFERENCES

- [1] A. M. Gabor, J. R. Tuttle, D. S. Albin, A. L. Tennant, M. A. Contreras, and R. Noufi, in *Proc. 12th NREL P. V. Program Review Meeting*, Oct. 13-15, 1993, Denver, CO (AIP, 1994).
- [2] M. A. Contreras, et al., to appear in *Progress in Photovoltaics*.
- [3] J. R. Tuttle, M. A. Contreras, J. S. Ward, A. M. Gabor, K. R. Ramanathan, A. L. Tennant, L. Wang, J. Keane, and R. Noufi, "High efficiency Cu(In,Ga)Se₂-based thin-film solar cells: 16.8% total-area one-sun and 17.2% total-area 22-sun device performance," *this conference*.
- [4] *2nd EPRI Sponsored Workshop on CuInSe₂ Materials*, Estes Park, CO, October 17-19, 1993, unpublished.
- [5] T. J. Vink, et al., "Stress, strain, and microstructure of sputter-deposited Mo thin films," *J. Appl. Phys.* **70**, 4301-8 (Oct. 1991).
- [6] J. H. Scofield, A. Duda, D. Albin, B. L. Ballard, and P. K. Predicki, "Sputtered molybdenum bilayer back contact forcopper indium diselenide-based polycrystalline thin-film solarcells," to appear in *Thin Solid Films*.

- [7] J. Hedström, H. Ohlsén, M. Bodegård, A. Kylner, and L. Stolt, "ZnO/CdS/Cu(In,Ga)Se₂ thin film solar cells with improved performance," *Proceedings 23rd IEEE Photovoltaics Specialists Conference*, Louisville, KY (IEEE, New York, 1993) pp. 364-71.